The Link between Ion Permeation and Inactivation Gating of Kv4 Potassium Channels

Mohammad Shahidullah and Manuel Covarrubias
Department of Pathology, Anatomy and Cell Biology, Jefferson Medical College of Thomas Jefferson University, Philadelphia, Pennsylvania 19107

ABSTRACT   Kv4 potassium channels undergo rapid inactivation but do not seem to exhibit the classical N-type and C-type mechanisms present in other Kv channels. We have previously hypothesized that Kv4 channels preferentially inactivate from the preopen closed state, which involves regions of the channel that contribute to the internal vestibule of the pore. To further test this hypothesis, we have examined the effects of permeant ions on gating of three Kv4 channels (Kv4.1, Kv4.2, and Kv4.3) expressed in *Xenopus* oocytes. Rb^+ is an excellent tool for this purpose because its prolonged residency time in the pore delays K^+ channel closing. The data showed that, only when Rb^+ carried the current, both channel closing and the development of macroscopic inactivation are slowed (1.5- to 4-fold, relative to the K^+ current). Furthermore, macroscopic Rb^+ currents were larger than K^+ currents (1.2- to 3-fold) as the result of a more stable open state, which increases the maximum open probability. These results demonstrate that pore occupancy can influence inactivation gating in a manner that depends on how channel closing impacts inactivation from the preopen closed state. By examining possible changes in ionic selectivity and the influence of elevating the external K^+ concentration, additional experiments did not support the presence of C-type inactivation in Kv4 channels.

INTRODUCTION

Gated ion channels that control the passive transport of ions across biological membranes respond to chemical and physical stimuli by undergoing conformational changes that open their ion-selective pore. Thus, the basic operation of an ion channel depends on the combination of two separate processes: gating and ion permeation. These processes, however, are not independent. Most likely, ions move through a long pore within the channel and interact with parts that undergo conformational changes as the channel opens, closes, and inactivates. Various studies have examined this hypothesis and have provided strong evidence of a reciprocal interaction between permeant ions and the gating machinery in voltage-gated ion channels (e.g., Swenson and Armstrong, 1981; Matteson and Swenson, 1986; Demo and Yellen, 1992; Gomez-Lagunas and Armstrong, 1994; Baukrowitz and Yellen, 1995; Chen et al., 1997; Zheng and Sigworth, 1997; Ogielska and Aldrich, 1999; Townsend et al., 1997; Zheng et al., 2001). For instance, in *Shaker* K^+ channels, elevated external K^+ slows C-type inactivation and promotes the recovery from N-type and C-type inactivation (Demo and Yellen, 1991; Lopez-Barneo et al., 1993; Levy and Deutsch, 1996a,b). Thus, K^+ probably modulates C-type inactivation at an external site, and N-type inactivation involves a direct occlusion of the pore at an internal site. Also, C-type inactivation in these channels is faster when the pore becomes vacant as a result of the occlusion of the inner mouth of the pore by the N-type inactivation gate (Baukrowitz and

Yellen, 1995). This result suggested that the ionic occupancy of the pore determines the rate of C-type inactivation. Reinforcing the relationship between ion permeation and inactivation gating, some K^+ channels become impermeable to K^+ and relatively more Na^+ permeable when they undergo C-type inactivation (Starkus et al., 1997; Kiss et al., 1999). Such a change in ionic selectivity is consistent with a mechanism of C-type inactivation involving a concerted conformational change at the selectivity filter of some Kv channels (Ogielska et al., 1995; Panyi et al., 1995; Liu et al., 1996; Loots and Isacoff, 1998).

K^+ channel deactivation is also influenced by permeant ions. In a seminal study, Swenson and Armstrong (1981) discovered that squid axon K^+ channels close more slowly in the presence of elevated concentrations of K^+ or when Rb^+ carries the inward current through the pore. These authors hypothesized that when Rb^+ or K^+ occupies the pore, the activation gate may have difficulty closing. Importantly, Rb^+ interfered with channel closing more effectively because it exhibits a prolonged residency time in the pore (Eisenman et al., 1986; Demo and Yellen, 1992; Morais-Cabral et al., 2001). In agreement with the "occupancy hypothesis," further observations showed that only permeant ions affect gating and that these interactions involve a pore site (Matteson and Swenson, 1986; Sala and Matteson, 1991). Similarly, the hypothetical mechanism of C-type inactivation assumes that the presence of K^+ in the selectivity filter interferes with a presumed partial collapse of the pore by a "foot-in-the-door" mechanism (Yeh and Armstrong, 1978; see above).

The ionic and kinetic bases of fast and slow inactivation in *Shaker* K^+ channels have been extensively investigated and are relatively well understood (Yellen, 1998; 2001). By contrast, the mechanisms of inactivation of Kv4 channels

differ from those known in *Shaker* K$^+$ channels, and recent studies are beginning to provide insights into the molecular basis of Kv4 inactivation (Jerng and Covarrubias, 1997; Jerng et al., 1999; Bähring et al., 2001; Beck and Covarrubias, 2001; Beck et al., 2002). From those studies a novel hypothesis proposes that the opening equilibrium is backward-biased or weakly forward-biased in Kv4 channels and, consequently, significant inactivation from the preopen inactivation-permissive closed state is coupled to channel closing at all relevant membrane potentials. An important prediction of this hypothesis is that variables that influence channel closing affect the maximum open probability (expected to be low) and exert a parallel effect on the development of inactivation because the observed rate of inactivation depends on the occupancy of the preopen closed state.

Here, we have further probed the mechanisms of inactivation of Kv4 channels by examining how certain permeant cations influence gating of all mammalian Kv4 channels (Kv4.1, Kv4.2, and Kv4.3). Resorting to the "occupancy hypothesis," we found that, when Rb$^+$ is the current carrying ion in all Kv4 channels, both the development of deactivation and inactivation are slowed and the peak currents are increased. Thus, when Rb$^+$ occupies the pore the activation gate has difficulty closing and the maximum open probability increases, which indirectly delays closing of a putative internal inactivation gate (Jerng et al., 1999). This explanation is consistent with the presence of preferential inactivation from the preopen closed state. We also examined the development of inactivation in the absence of external K$^+$ (complete substitution with Na$^+$) and in the presence of low concentrations of internal K$^+$ or no added internal K$^+$. This experiment revealed that, in contrast to other Kv channels, the relative Na$^+$ permeability of Kv4.1 channels does not increase during the development of inactivation, which rules unlikely the presence of C-type inactivation. Accordingly, elevated external K$^+$ accelerated inactivation of all Kv4 channels (opposite to the effect on C-type inactivation in *Shaker* K$^+$ channels; Lopez-Barneo et al., 1993; Ogielska and Aldrich, 1999). Preliminary reports of this study were previously published in abstract form (Covarrubias et al., 2000; Shahidullah and Covarrubias, 2001).

MATERIALS AND METHODS

Molecular biology and cRNA microinjection

Mouse Kv4.1 is maintained in pBluescript II KS (Strategene, La Jolla, CA). Kv4.2 and Kv4.3 cDNAs (from rat) were kindly provided by Dr. J. Nerbonne (Washington University, St. Louis, MO), and are maintained in pRc/CMV (Invitrogen, Carlsbad, CA) and pBK-CMV (Strategene, La Jolla, CA), respectively. Kv1.3 cDNA in pGEM-9z (Promega, Madison, WI) was a gift from Dr. Carol Deutsch (University of Pennsylvania, Philadelphia, PA). Capped cRNA for expression in *Xenopus* oocytes was produced by in vitro transcription using the Message Machine Kit (Ambion, Austin, TX).

cRNAs were injected into defolliculated *Xenopus* oocytes ($\leq$50 ng/cell) using a Nanoject microinjector (Drummond, Broomall, PA). Currents were recorded two to seven days postinjection.

Electrophysiology

Patch-clamp recording was conducted as described before (Jerng et al., 1999; Beck and Covarrubias, 2001) using an Axopatch 200A or 200B amplifier (Axon Instruments, Foster City, CA). All experiments were conducted with inside-out patches (except Fig. 11). Patch pipettes were constructed from Corning glass 7052 or 7056 (Warner Instrument Corp., Hamden, CT). For the recording of fast macroscopic currents (e.g., tail relaxations) and single-channel currents, the pipettes ($\sim$0.5–1 MΩ and 10–20 MΩ in the bath solution, respectively) were coated with Sylgard elastomer (Dow Corning Co. Midland, MI). For experiments in Fig. 10, the pipette solution contained (Kiss et al., 1999; mM): 165 Na, 2 CaCl$_2$, 1 MgCl$_2$, 10 Glucose, 20 HEPES (pH 7.3, adjusted with NaOH); and the internal bath solution contained (Kiss et al., 1999; mM): 140 XCl (X = K$^+$ or N-methyl-D-glucamine (NMDG$^+$)), 1 CaCl$_2$, 10 EGTA, 2 MgCl$_2$, 20 HEPES (pH 7.3). For experiments in Fig. 11, the pipette solution contained (mM): 96 XCl (X = Na$^+$ or K$^+$), 2 KCl, 1 MgCl$_2$, 1.8 CaCl$_2$, 5 HEPES (pH 7.4, adjusted with NaOH); and the internal bath solution contained (mM): 98 KCl, 0.5 MgCl$_2$, 1 EGTA, 10 HEPES (pH 7.2, adjusted with KOH). To examine Rb$^+$ currents, RbCl was replaced for KCl in the solution described above. These solutions were used in all other experiments (Figs. 1–9) under symmetrical (K/K and Rb/Rb), or bi-ionic conditions (K/Rb and Rb/K). A two-barreled theta tube was used to constantly expose the internal side of the patches to K$^+$ or Rb$^+$. The open end of the theta tube ($\sim$300 μm) was placed within 100 μm from the tip of the patch pipette, which was manually moved to expose the patch to a laminar flow of the desired solution. Under bi-ionic conditions (e.g., K_{out}/Rb_{in}), the reversal potential for Kv4.1 currents was +8 $\pm$ 1 mV ($n = 5$) and the permeability ratio (P_{Rb}/P_K) was 0.73, which agrees with values estimated by others for Kv channels (e.g., Sala and Matteson, 1991; Ding and Horn, 2002). The passive leak current and the capacitive transients were subtracted on-line using a P/4 procedure. The capacitive transients and the passive leak current from single-channel records were removed by subtracting blank sweeps (no unitary currents) from active traces. The complex kinetics of Kv4 unitary currents (Results and Fig. 3; Jerng et al., 1999; Beck et al., 2002; Holmqvist et al., 2002) are unlikely to result from contaminating endogenous channels or patch breakdown because *1*) they are mainly observed in bursts of channel activity near the first half of the test pulses, *2*) they are associated with the expression of Kv4 channels (Kv4.1 and Kv4.3), and *3*) they are not apparent in patches from uninjected oocytes and oocytes expressing other Kv channels (Shaw2 and Kv3.4). The recordings were filtered at 0.5–1.5 kHz (-3 db, 8-pole Bessel filter; Frequency Devices, Haverhill, MA) and digitized at 2–10 kHz. All experiments were recorded at room temperature (23 $\pm$ 1°C).

Data acquisition and analysis

A Pentium class computer interfaced to a 12-bit A/D converter (Digidata 1200 using Clampex 7.0 or 8.0; Axon Instruments, Foster City, CA) controlled the voltage-clamp protocols and data acquisition. Data analysis was conducted using Clampfit 8.0 (Axon Instruments), and Origin 6.0 or 7.0 (OriginLab Corp., Northhampton, MA). Current relaxations and other time-dependent processes were described assuming a simple exponential function or the sum of exponential terms (Jerng and Covarrubias, 1997). The time constants of deactivation and inactivation were assumed to depend exponentially on membrane potential according to this relation: $\tau(V) = \tau(0) \exp(\pm qV/kT)$, where $\tau(V)$ is the time constant at a given membrane potential V, q is the apparent charge associated with the process under investigation, k is the Boltzmann constant and T is the absolute temperature. Using the pClamp 8.0 analysis software (Axon Instruments), a standard half-way threshold criterion was applied to idealize the single-channel records. The resulting event list was then used to construct amplitude and dwell-time
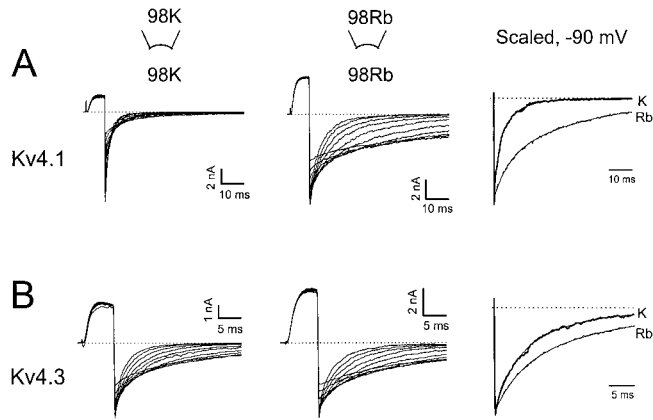
FIGURE 1 Rb^+ tail currents exhibit slower deactivation. (*A*) and (*B*) Inward Kv4.1 and Kv4.3 tail currents evoked by pulses ranging between -140 and -50 mV, after evoking the outward current by a depolarization to $+50$ mV from a holding potential of -100 mV. Currents are recorded from inside-out patches containing symmetrical 98 mM K^+ (*A, left*) or symmetrical 98 mM Rb^+ (*B, middle*; see also Materials and Methods). (*A, right*) and (*B, right*) Scaled tail currents, -90 mV. Thick lines, 98 mM K^+, and thin lines, 98 mM Rb^+. Dashed lines in all panels mark the zero current level. The solid lines superimposed on the scaled tail current traces represent the best biexponential fits with the following parameters for Kv4.1: τ_F (K/K) = 2.9 ms, τ_S (K/K) = 13.4 ms, A_F/A_S (K/K) = 2.8, τ_F (Rb/Rb) = 5.5 ms, τ_S (Rb/Rb) = 39 ms, and A_F/A_S (Rb/Rb) = 0.5; and the following parameters for Kv4.3: τ_F (K/K) = 2.9 ms, τ_S (K/K) = 12.1 ms, A_F/A_S (K/K) = 0.7, τ_F (Rb/Rb) = 4.5 ms, τ_S (Rb/Rb) = 22.4 ms, and A_F/A_S (Rb/Rb) = 0.6.

histograms, and a Simplex maximum likelihood method was applied to fit sums of exponentials to the logarithmically transformed distributions of dwell times (pSTAT, Axon Instruments). Unless indicated otherwise, all measurements were expressed as mean $\pm$ SE. The Student's t-test or one-way ANOVA were used to evaluate the statistical significance of the observed differences (p-values are given in the text, tables, and figure legends). Tukey box plots were used to demonstrate data dispersion in Figs. 4, 9, and 11. The lower and upper borders of the box represent the 25th and 75th percentiles, respectively; and the whiskers correspond to the 1st and 99th percentiles. The line across the box represents the 50th percentile and the solid circle marks the mean value. The open circles represent the extreme values. The peak chord conductance Gp was computed as $Gp = Ip / (V - Vr)$, where Ip is the peak current, V is the command voltage and Vr is the reversal potential, which was determined from each individual experiment. The instantaneous current–voltage relation obtained in the presence of symmetrical K^+ (not shown) exhibited a modest inward rectification. Thus, to examine the majority of the experiments only the inward currents in the linear regime of the instantaneous current voltage relation (-100 to -10 mV; Fig. 5 *C*) were included in the analysis. A limited number of corrected activation curves ($I_{PEAK}/I_{INSTANTANEOUS}$, -100 to $+60$ mV) were also constructed to confirm the validity of this analysis (Fig. 5 legend). The Gp-V curves were described assuming a fourth-order Boltzmann function (Beck and Covarrubias, 2001). The $V_{1/2}$ obtained from this function is the midpoint potential for the activation of one subunit, which approximately corresponds to the apparent "threshold" voltage of activation, and k is the corresponding slope factor (per e-fold change).

RESULTS

Rb^+ currents through Kv4 channels exhibit slower deactivation

A previous mutational analysis of inactivation gating in Kv4.1 channels suggested a parallel relationship between
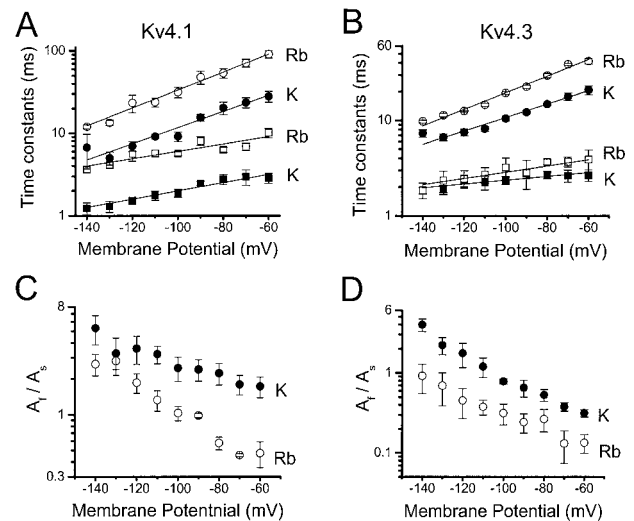
FIGURE 2 Deactivation kinetics of Kv4 tail current mediated by K^+ or Rb^+. Data were analyzed as described in Fig. 1 legend. (*A*) and (*B*) Voltage-dependence of the slow (*circle*) and fast (*square*) time constants of deactivation from Kv4.1 and Kv4.3 channels. Solid and open symbols are from K^+ and Rb^+ currents, respectively. Lines across the symbols are the best-fit exponentials that describe the voltage-dependence of the time constants (Materials and Methods). The partial charges derived from these fits are listed in Table 1. (*C*) and (*D*) Voltage-dependence of the corresponding amplitude ratio A_F/A_S derived from the biexponential fits. All symbols are the means from three to seven experiments.

inactivation and channel closing (Jerng et al., 1999), which could not be explained if inactivation were to occur mainly from the open state. Thus, it was predicted that slowing channel closing by other means must also slow inactivation because the channel must close before inactivating. Rb^+ and other permeant ions affect gating by acting at a site in the pore (Swenson and Armstrong, 1981; Matteson and Swenson, 1986; Sala and Matteson, 1991). The "occupancy hypothesis" proposes that a permeant ion with a long residency time in the permeation pathway (e.g., Rb^+) can hinder channel closing. To study whether this paradigm can be applied to test the relationship between inactivation and channel closing, the deactivation of Kv4.1 and Kv4.3 channels was first investigated by examining the kinetics of tail currents at various membrane potentials (Figs. 1 and 2). Inside-out patches were exposed to symmetric 98 mM K^+, or symmetric 98 mM Rb^+. The channels generated well-resolved tail current relaxations mediated by K^+ or Rb^+ and,

TABLE 1 **Apparent charges derived from the kinetics of deactivation**

Parameter	Permeant ion	Kv4.1	Kv4.3
τ_{SLOW}	K^+	0.57	0.42
τ_{SLOW}	Rb^+	0.63	0.5
τ_{FAST}	K^+	0.29	0.12
τ_{FAST}	Rb^+	0.26	0.19

The apparent charges (q) were extracted from the analysis presented in Fig. 2.
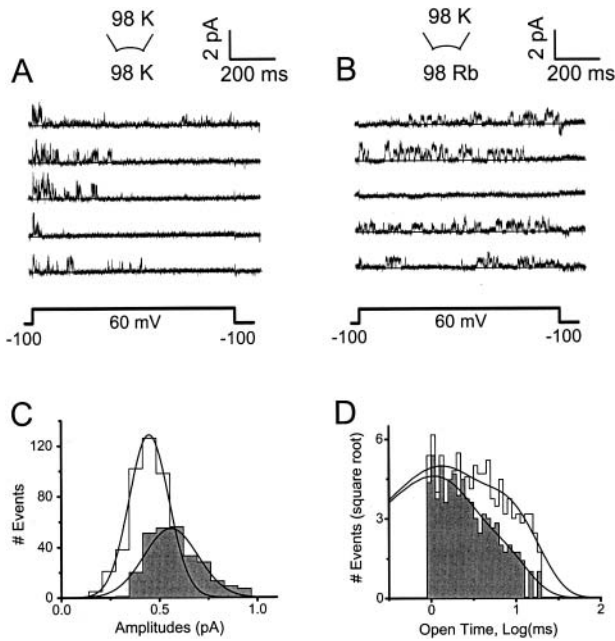
FIGURE 3   Rb$^+$ reduces the unitary amplitude and increases the mean open time of Kv4.1 channels. (*A*) and (*B*) Consecutive Kv4.1 unitary current traces evoked by the pulse protocol shown in the lower part of these panels. Both recordings are from the same inside-out patch. K$^+$ (symmetric 98 mM K$^+$) or Rb$^+$ (bi-ionic conditions) mediated the currents. Recordings were low-pass filtered at 1.5 kHz and digitized at 5 kHz. The solid line across the traces represents the zero current level. (*C*) Amplitude histogram derived from the complete data set sampled in *A* and *B*. Shaded and unshaded histograms are from K$^+$ and Rb$^+$ currents, respectively. The solid lines represent the best-fit Gaussian functions with the following parameters: $\mu = 0.56$ pA and $\sigma = 0.13$ pA, for the K$^+$ currents; $\mu = 0.45$ pA and $\sigma = 0.1$ pA, for the Rb$^+$ currents (μ and σ are the mean and standard deviation, respectively). (*D*) Histogram of open intervals derived from the complete data set sampled in *A* and *B*. Shaded and unshaded histograms are from K$^+$ and Rb$^+$ currents, respectively. The solid lines represent the best-fit biexponential functions with the following parameters: $\tau_{LONG} = 3.2$ ms, $w_{LONG} = 0.3$, $\tau_{BRIEF} = 0.9$ ms, and $w_{BRIEF} = 0.7$ for K$^+$ currents; $\tau_{LONG} = 7$ ms, $w_{LONG} = 0.4$, $\tau_{BRIEF} = 1$ ms, and $w_{BRIEF} = 0.6$ for Rb$^+$ currents (τ and w are the mean open time and the relative weight, respectively). Average values from different patches are given in Table 2.

as expected, the Rb$^+$ tail currents were significantly slower (Fig. 1). A sum of two exponential terms was assumed to describe the current relaxations (Figs. 1 and 2; Fig. 1 legend). Rb$^+$ significantly increased the time constants of the tail currents, even though Kv4.1 currents exhibited a larger effect than Kv4.3 currents (Fig. 2). Both fast and slow time constants increased with membrane depolarization, but the slow time constant was more voltage-dependent (Fig. 2, *A* and *B*). The voltage-dependencies of both time constants were, however, similar for K$^+$ and Rb$^+$ currents (the relations for K$^+$ and Rb$^+$ in Fig. 2, *A* and *B* are approximately parallel). The apparent electronic charges were estimated assuming that the time constants depend exponentially on voltage (Materials and Methods; Fig. 2; Table 1). These values are consistent with the weak voltage-dependence of channel closing reported for Kv channels (e.g., Zagotta et al., 1994; Schoppa and Sigworth, 1998). The

TABLE 2   Single-channel properties of Kv4.1 channels

Parameter*	K$^+$ current	Rb$^+$ current	$P^{\ddagger}$
Mean current at +60 mV (pA)	0.56 ± 0.04 ($n = 6$)	0.41 ± 0.03 ($n = 6$)	0.02
τ_O, brief (ms)	0.9 ± 0.01 ($n = 3$)	1.1 ± 0.2 ($n = 4$)	0.4
τ_O, long (ms)	4.4 ± 0.8 ($n = 3$)	7.1 ± 0.5 ($n = 4$)	0.03
W_O, brief	0.82 ± 0.06 ($n = 3$)	0.64 ± 0.03 ($n = 4$)	0.03
W_O, long	0.18 ± 0.05 ($n = 3$)	0.38 ± 0.03 ($n = 4$)	0.02

*τ_O is the mean open duration and W_O is the relative weight.
‡*t*-Student statistics.

amplitude ratio (A_F/A_S) of the exponential terms also decreased in a voltage-dependent manner as the contribution of the slow component increased with membrane depolarization (Fig. 2, *C* and *D*). Overall, these observations are consistent with the "occupancy hypothesis" in Kv4 channels by showing that Rb$^+$ in the permeation pathway hinders closing of the pore. The presence of two time constants of deactivation also suggests that closing of Kv4 channels involves at least two steps (Discussion). Rb$^+$ slows both steps (especially in Kv4.1) and decreases the A_F/A_S ratio (only the voltage-dependence of the Kv4.1 A_F/A_S ratio appeared modestly increased by Rb$^+$; Fig. 2 *C*). Thus, Rb$^+$ favors the slow process, which namely accounts for the slower deactivation of the Rb$^+$ currents. Bähring et al. (2001) obtained qualitatively similar results from the K$^+$ and Rb$^+$ tail currents generated by Kv4.2 channels expressed in HEK-293 cells. Their analysis, however, only described one voltage-dependent time constant of deactivation (involving an apparent charge of ~ 0.5 e_0).

Rb$^+$ enhances Kv4 currents by stabilizing the open state

Unitary Kv4.1 currents mediated by K$^+$ or Rb$^+$ were compared to verify the prolonged pore residency time of Rb$^+$ and the resulting stabilization of the open state (Fig. 3). Kv4.1 was chosen for these experiments because it exhibited the relatively larger effects described above (Figs. 1 and 2). As demonstrated previously (Jerng et al., 1999; Beck et al., 2002; Holmqvist et al., 2002), Kv4 unitary currents mediated by K$^+$ show rapid and complex gating and at least two conductance levels (Fig. 3 *A*). Because the channels inactivate quickly when K$^+$ mediates the current, the greatest single-channel activity was observed during the first third of the test pulse (+60 mV). From the same patch (after replacing internal K$^+$ with Rb$^+$), unitary Rb$^+$ currents at the same membrane potential appeared smaller and exhibited slower gating with activity that spread across the length of the pulse because a slower development of inactivation (Fig. 3 *B*). A detailed kinetic analysis of unitary currents is outside of the scope of this study. However, unitary currents that crossed a 50% threshold (Materials and Methods) were examined to estimate the mean unitary
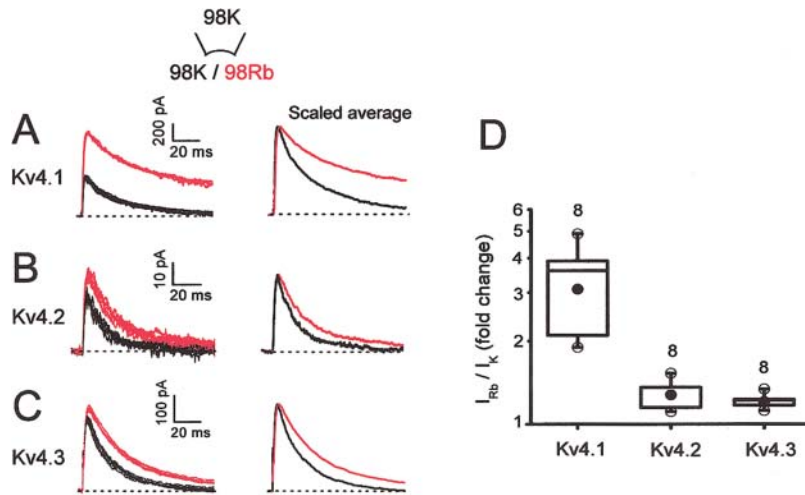
FIGURE 4   Rb$^+$ potentiates Kv4 currents. (*A–C*) Kv4.1, Kv4.2, and Kv4.3 currents evoked by repetitive step depolarizations to +50 mV from a holding potential of −100 mV. Inside-out patches were exposed to symmetric or bi-ionic conditions by switching the internal solution from 98 mM K$^+$ (*black traces*) to 98 mM Rb$^+$ (*red traces*). The pipette solution was 98 mM K$^+$ (Materials and Methods). Scaled averaged outward currents are also shown (*right panel*; six to seven traces from each condition). (*D*) Box plots (Materials and Methods) comparing the fold change in the peak currents.

current and mean open time. If Rb$^+$ exhibits a prolonged residency time in the pore of Kv4.1 channels, the mean unitary current should decrease and, consequently (if Rb$^+$ stabilizes the open state), the mean open time should increase. Accordingly, the mean unitary Rb$^+$ current at +60 mV was ~27% smaller than the corresponding K$^+$ current (Fig. 3 *C*; Table 2). The distribution of open dwells was well described by the sum of two exponential terms (Fig. 3 *D*), which suggests the presence of two open states with similar single-channel conductances. The mean open time of the brief openings was ~1 ms and was not significantly changed by Rb$^+$ (Table 2). In contrast, the mean open time of the long openings was ~4 ms and was prolonged by ~60% when Rb$^+$ mediated the current (Table 2). Also, Rb$^+$ approximately doubled the relative contribution of the long openings to the distribution of open dwells (Table 2). The complex kinetics of the unitary currents precluded a direct assessment of the peak open probability because the number of channels in a patch could not be estimated.

A more stable open state might increase the magnitude of the macroscopic current by increasing the open probability. Accordingly, the outward peak Rb$^+$ currents were significantly greater than the corresponding K$^+$ currents (Fig. 4). In these experiments, outward K$^+$ and Rb$^+$ currents were studied in the same patch by repetitively switching between K$^+$- and Rb$^+$-containing solutions (98 mM), which showed that the effects are reversible and that there is no drift in the recordings. In the Rb$^+$-containing internal solution, Kv4.1 currents exhibited the largest increase (~threefold) and Kv4.2 and Kv4.3 exhibited smaller but significant increases (~1.25-fold). Qualitatively, these changes reflect the relative changes in deactivation kinetics (see above; see also Figs. 1 and 2). Interestingly, Kv1.3 outward currents measured under similar conditions were suppressed (~36%) despite slower deactivation when Rb$^+$ mediates the tail currents (data not shown). In this case, the reduced unitary conductance of the Rb$^+$ currents might be the dominant factor that determines the Kv1.3 macroscopic current.

The rising phase of the currents evoked by a depolarization to +60 mV was examined to test the effect of Rb$^+$ on current activation. The $t_{50\%}$ values (time to 50% of the rising phase) were 1.5 ± 0.2 ms and 1.7 ± 0.2 ms ($n = 6$) when K$^+$ and Rb$^+$ mediated the outward currents, respectively. Thus, Rb$^+$ does not significantly affect the kinetics of current activation. The peak conductance-voltage (*Gp-V*) relations derived from currents measured in symmetrical K$^+$ or symmetrical Rb$^+$ (98 mM) was also examined to test the relative effect of Rb$^+$ on voltage-dependent activation (Fig. 5). The normalized *Gp-V* curve from the Rb$^+$ currents appeared leftward shifted ($\Delta V_{G=50\%} = -10$ mV; Fig. 5 legend). Strictly speaking, the *Gp-V* curve of Kv4 channels cannot be interpreted as the activation curve, because its shape is strongly influenced by fast inactivation (Beck and Covarrubias, 2001). Nevertheless, the observed changes of the *Gp-V* curve are consistent with a relatively more stable open state and reduced inactivation. It is also notable that under both ionic conditions the projected maximum *Gp* has already been reached at +60 mV (the test voltage that examined the effect of Rb$^+$ on the magnitude of the macroscopic currents; Fig. 4 and corresponding legend). Thus, a simple modest shift of the *Gp-V* curve is not sufficient to explain the larger Rb$^+$ currents described above. Most likely, Rb$^+$ also influences the maximum open probability of Kv4 channels, which is determined by transitions near the open state(s) (Discussion). Under bi-ionic conditions (98 mM, K_{out}/Rb_{in}), Rb$^+$ did not alter the voltage-dependence of the inward K$^+$ current (all Kv4 channels). Thus, an effect of Rb$^+$ on channel gating that is independent of permeation is unlikely. Rb$^+$ alters gating when it acts as the current-carrying ion (see below).

Rb$^+$ permeation delays inactivation of Kv4 currents

Assuming that channels mainly inactivate from the open state, the observed rate of inactivation should increase if the open probability increases as a result of slower channel
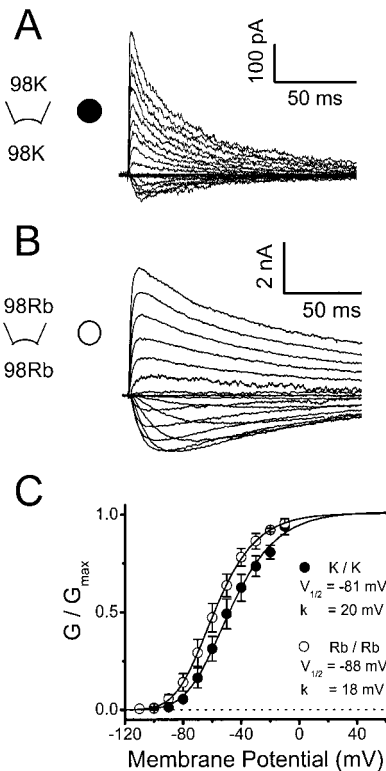
FIGURE 5   Peak conductance–voltage relation of Kv4.1 channels under symmetrical ionic conditions. (*A*) and (*B*) Kv4.1 K$^+$ and Rb$^+$ currents evoked by step depolarizations to various voltages ranging between -100 and $+60$ mV in 10-mV intervals. The holding potential was -100 mV. In both instances the currents were recorded from inside-out patches exposed to symmetrical 98 mM K$^+$ or 98 mM Rb$^+$. The reversal potentials under these conditions were -0.5 ± 0.9 mV and -0.6 ± 1.0 mV, in symmetrical K$^+$ or symmetrical Rb$^+$, respectively. (*C*) Normalized peak conductance-voltage relation (Materials and Methods). Lines are the best-fit fourth-order Boltzmann functions (Materials and Methods) with the parameters indicated in the graph. The graphically interpolated voltages that activate 50% of the peak conductance ($V_{G=50\%}$) were -50 mV and -60 mV in symmetrical K$^+$ and symmetrical Rb$^+$, respectively. Symbols are the means from three to six experiments. From pooling the best-fit parameters extracted from these experiments the mean $V_{1/2}$ values were -78 ± 3 mV and -86 ± 3 mV in symmetrical K$^+$ and symmetrical Rb$^+$, respectively; and the mean k values were 18 ± 1 mV and 17 ± 1 mV in symmetrical K$^+$ and symmetrical Rb$^+$, respectively. The analysis of a limited number of corrected activation curves ($n = 3$, Materials and Methods) generated more variable curves but similar values of the extracted activation parameters: the mean $V_{1/2}$ values were -78 ± 3 mV and -83 ± 4 mV in symmetrical K$^+$ and symmetrical Rb$^+$, respectively; and the mean k values were 17 ± 2 mV and 21 ± 2 mV in symmetrical K$^+$ and symmetrical Rb$^+$, respectively.

closing. In contrast, the results in Figs. 3–6 show that the development of macroscopic inactivation of Rb$^+$ currents was significantly slowed (along with slower channel closing; see above). Bähring et al. (2001) also reported slower inactivation of Kv4.2 channels in the presence of symmetrical Rb$^+$. Importantly, however, the experiments reported here also show that under bi-ionic symmetrical conditions (98 mM, K_{out}/Rb_{in}; Fig. 6), only the outward currents mediated by Rb$^+$ were slower, whereas, the inward currents mediated by K$^+$ were not affected by the presence of Rb$^+$

inside (Fig. 6, *A–C*; scaled currents at $+50$ and -30 mV). This effect was greater for Kv4.1 than for Kv4.2 or Kv4.3, which is reminiscent of the relative differences between peak currents and deactivation of K$^+$ and Rb$^+$ currents (Figs. 1–3). Relative to the peak current, the degree of inactivation was computed at the time of the maximal difference between K$^+$ and Rb$^+$ currents (degree of inactivation = current at time of maximal difference / peak current). For instance, this estimate yielded a three- to fourfold slower inactivation of the Kv4.1 Rb$^+$ currents, a change that is similar to that determined from deactivation of the tail currents.

The development of inactivation in all instances was well described by the sum of two exponential terms. Under symmetrical K$^+$ conditions (98 mM), slow and fast time constants differing by greater than threefold were clearly resolved and exhibited little or no voltage-dependence (Fig. 7, *A–C*). The corresponding amplitude ratios (A_F/A_S) appeared more variable, exhibited little or no voltage dependence, and ranged between 0.2 and 3 (Fig. 7, *D–F*). When Rb$^+$ mediated the outward currents under bi-ionic conditions (see above), the fast and slow time constants of inactivation were greater than those measured from the K$^+$ currents and increased in a voltage-dependent manner between $+10$ and $+60$ mV (Fig. 7 *A–C*). The apparent charges associated with the voltage-dependence of the slow time constants were ~ 0.4 e_0, ~ 0.3 e_0, and ~ 0.5 e_0 for Kv4.1, Kv4.2, and Kv4.3, respectively. The amplitude ratio (A_F/A_S) of Rb$^+$ currents mediated by Kv4.1 appeared to decrease slightly, but that of Kv4.2 and Kv4.3 was more variable and displayed no significant change (Fig. 7, *D–F*).

The novel voltage-dependence of the time constants of inactivation is a reflection of how the electrochemical gradient influences ion occupancy in the pore and, consequently, closing and inactivation of Kv4 channels (Discussion). Accordingly, when the ionic gradients were reversed (Rb_{out}/K_{in}) the inward Kv4.1 Rb$^+$ currents also exhibited a novel and opposite voltage-dependence that is not apparent in symmetrical K$^+$ or symmetrical Rb$^+$ (Fig. 8). The apparent charge derived from this voltage-dependence was similar to that of the outward currents (~ 0.7 e_0). These results strongly suggest that ion permeation influences inactivation gating of Kv4 channels. As proposed earlier for all Kv4 channels (Jerng et al., 1999; Bähring et al., 2001; Beck and Covarrubias, 2001; Beck et al., 2002), the parallel effects of Rb$^+$ permeation on the development of inactivation and channel closing are more consistent with a pathway of inactivation originating from a preopen closed state (Discussion).

Rb$^+$ does not affect Kv4 closed-state inactivation at hyperpolarized membrane potentials

The results shown so far demonstrate that whenever Rb$^+$ is the current carrying ion, both the development of de-activation and inactivation are slowed. This relationship suggests that channel closing indirectly controls inactivation
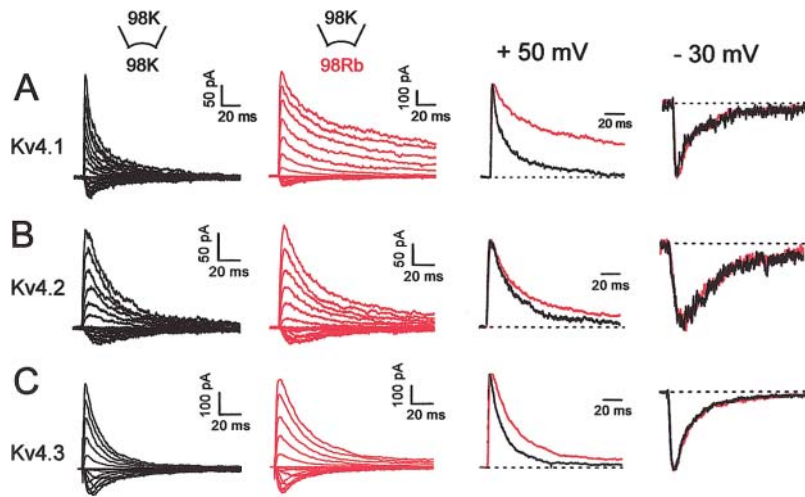
FIGURE 6 Inactivation of Kv4 currents under symmetrical (K_{out}/K_{in}) and bi-ionic conditions (K_{out}/Rb_{in}). (*A–C*) Kv4 currents expressed in inside-out patches were evoked as detailed in Fig. 5 legend. (*First column*) In symmetrical 98 mM K^+. (*Second column*) The same patch after switching the internal bath solution to 98 mM Rb^+. (*Third column*) Scaled outward currents from the first and second columns at +50 mV (currents mediated by K^+ (*black*) or Rb^+ (*red*). (*Fourth column*) scaled inward currents from the first and second columns at −30 mV (both currents are mediated by K^+). Dashed lines indicate the zero current level.

from a preopen closed state. Could Rb^+ also hinder Kv4 inactivation by a direct interaction? Lopez-Barneo et al. (1993) proposed that external permeant ions may directly impede both open- and closed-state inactivation at a pore site in *Shaker* K^+ channels, and thereby they simultaneously slow the development of inactivation and increase the magnitude of the outward current. To test whether Rb^+ also slows inactivation from the closed state (before the channels have a chance to open), Fig. 9 compares the development of closed-state inactivation and recovery from inactivation at hyperpolarized membrane potentials (from −120 to −90 mV) for Kv4.1 in the presence of symmetrical K^+ or Rb^+ (98 mM). Elevated external K^+ (relative to 2 mM in inside-out patches; Beck and Covarrubias, 2001) accelerated closed-state inactivation by two- to threefold (at −90 mV), which contributes to a 15–20 mV hyperpolarizing shift of the prepulse inactivation curve (from −80 mV to −100 mV; Beck and Covarrubias, 2001 and Fig. 9 *D*). In symmetrical Rb^+ (relative to symmetrical K^+) the development of closed-state inactivation at −90 mV and the recovery from inactivation at −120 mV were not significantly affected ($p \geq 0.05$; Fig. 9, *A–C*). These results are in contrast to the effect of Rb^+ on the development of inactivation at more positive voltages (Figs. 6–8). Prepulse inactivation curves were also generated from the same patches used to measure the time courses of closed-state inactivation and recovery from inactivation. The curves were indistinguishable in the presence of symmetrical K^+ or Rb^+ (Fig. 9, *D–F*; including Kv4.2 and Kv4.3). Along with the rest of the observations, these results cannot be explained by simply assuming that permeant ions directly interact with a pore site to slow inactivation at positive voltages (that activate and open the channels) and leave inactivation unaffected at hyperpolarized voltages (not sufficient to open the channels significantly). The next two sections investigate more directly the possible contribution of the selectivity filter to the mechanisms of Kv4 inactivation.

Inactivation does not change the relative Na$^+$ permeability of Kv4.1 channels

The data presented so far and earlier studies have demonstrated that Kv4 channels undergo preferential closed-state inactivation (Jerng et al., 1999; Bähring et al., 2001; Beck and Covarrubias, 2001; Beck et al., 2002), but they may also inactivate from the open state, which might involve C-type inactivation. Recent studies showed that, when K^+ is completely replaced with Na^+ in the external solution and K^+ is low or absent in the internal solution, the development of slow inactivation in some Kv channels is associated with a decrease in K^+ permeability and an increase in the channel's relative permeability for Na^+ (Starkus et al., 1997; Kiss et al., 1999). To test whether a similar change contributes to inactivation of Kv4 channels, oocyte inside-out macropatches expressing Kv4.1 were exposed to 165 mM Na^+ in the pipette solution and various concentrations of K^+ in the internal solution (30 mM, 5 mM, and no added K^+). Currents were elicited by a step depolarization of increasing duration from a holding potential of −100 to +50 mV. Similar ionic conditions and pulse protocol were used by Kiss et al. (1999) to demonstrate the relative increase in Na^+ permeability when several Kv channels undergo C-type inactivation. Under these conditions, K^+ mediated the outward currents (if present, at +50 mV) and Na^+ mediated the inward tail currents (at −140 mV; Fig. 10, *A–C*). If an increase in the relative Na^+ permeability takes place, we expected an initial increase in the amplitude of the tail Na^+ currents as inactivation develops, which may then taper off as the channels underwent complete inactivation. With 30-mM internal K^+, the response to the shortest pulse (inducing little or no apparent inactivation) exhibited a significant inward tail current, demonstrating that Kv4.1 channels readily permeate Na^+ under the conditions of this experiment. As inactivation developed with longer pulses, the outward and inward
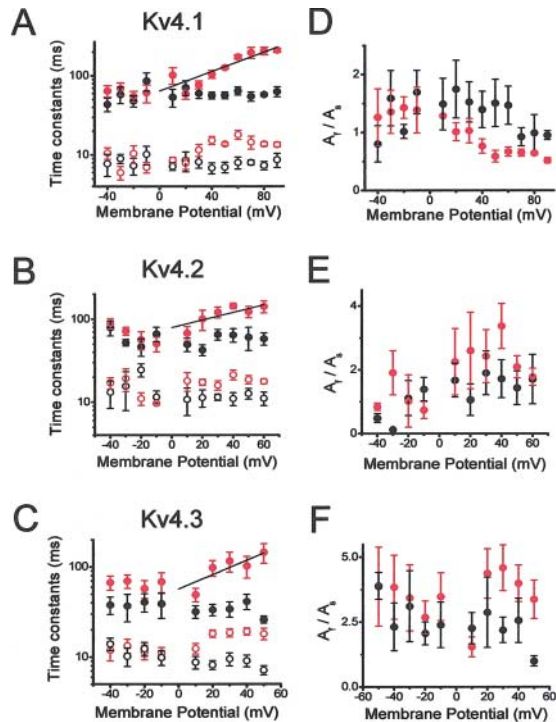
FIGURE 7 Kinetic analysis of the development of inactivation under symmetrical (K_{out}/K_{in}) and bi-ionic conditions (K_{out}/Rb_{in}). (*A–C*) Voltage-dependence of the time constants derived from the best-fit biexponential functions that described the development of macroscopic inactivation for Kv4.1, Kv4.2, and Kv4.3 channels. Ionic conditions were as described in Fig. 6 legend (*black symbols*, K_{out}/K_{in}; *red symbols*, K_{out}/Rb_{in}). Both ionic conditions were paired from the same patch. The line is the best-fit exponential that describes the voltage-dependence of the time constants derived from the development of inactivation of the Rb$^+$ currents (Materials and Methods). (*D–F*) Voltage-dependence of the corresponding amplitude ratio A_F/A_S derived from the biexponential fits. Symbols are the means from three to seven experiments.

currents declined following parallel time courses (Fig. 10 *A*). By plotting the outward current at the end of the depolarizing pulse and the corresponding inward peak tail currents as a function of the test pulse duration, and fitting exponential functions to the time courses (Fig. 10 *D*), it can be clearly seen that the decline of the peak tail Na$^+$ currents closely mirrors the decline of the outward K$^+$ currents ($\tau_{IN(Na)} = 90$ ms; $\tau_{OUT(K)} = 90$ ms). Furthermore, the channels remained highly selective for K$^+$ over Na$^+$. The reversal potentials were similar before inactivation develops and after 40% inactivation (-110 mV, not shown; corresponding to a $P_{Na}/P_K = 0.003$). Thus, it seems unlikely that the relative Na$^+$ permeability increases as inactivation develops in Kv4.1 channels. Although even in the presence of 30 mM K$^+$ in the internal solution, there was a significant Na$^+$ current before inactivation develops, internal K$^+$ might prevent a change in relative Na$^+$ permeability by blocking the inward Na$^+$ current (Starkus et al., 1997). Thus, the experiment was repeated in the presence of low internal K$^+$ (Fig. 10, *B* and *C* and *E* and *F*). With 5 mM K$^+$, there was also a significant Na$^+$ current before the onset of inactivation, and inactivation

was modestly faster, but the decline of the peak tail Na$^+$ currents simply mirrored the decline of the outward K$^+$ currents ($\tau_{IN(Na)} = 35$ ms; $\tau_{OUT(K)} = 25$ ms). When no internal K$^+$ was added, the experiment was more difficult because Kv4.1 channels did not seem to tolerate a prolonged absence of internal K$^+$ (in most attempts the currents run down). The limited results showed, however, no outward current (as expected) and the peak tail Na$^+$ current only appeared to decline monotonically with a $\tau_{IN(Na)}$ ~70 ms (two experiments gave similar results). In all cases, there were also no systematic changes in the kinetics of the Na$^+$ tail current as inactivation developed (data not shown). These results further support the absence of an increase in the relative Na$^+$ permeability associated with the development of inactivation. Independently of internal K$^+$, however, the amplitude of the peak tail Na$^+$ current remained relatively significant at steady state (at the end of the longest depolarization; Fig. 10, *D–F*).

Elevated external K$^+$ accelerates the development of inactivation in Kv4 channels

In *Shaker* K$^+$ channels, elevated external K$^+$ slows the development of inactivation and accelerates the recovery from inactivation (Lopez-Barneo et al., 1993; Levy and Deutsch, 1996). These effects are characteristic of the C-type mechanism of inactivation and appear to be related to the ionic occupancy of the pore (Baukrowitz and Yellen, 1995; Ogielska and Aldrich, 1999). In contrast, Kv4.1 channels in the presence of elevated external K$^+$ exhibit a slower recovery from inactivation, and inactivation of Kv4.1 and Kv4.2 channels develops at a faster rate (Jerng and Covarrubias, 1997; Kirichok et al., 1998; Bähring et al., 2001). To verify the latter result and extend the study to Kv4.3 (Eghbali et al., 2001), the development of macroscopic inactivation was investigated in cell-attached macropatches by exposing Kv4.1 or Kv4.3 channels to normal [K$^+$] (2 mM) or elevated [K$^+$] (98 mM) in the external solution (pipette; complete substitution of K$^+$ for Na$^+$). Clearly, the development of inactivation was faster in the presence of 98 mM K$^+$ (Fig. 11, *A* and *B*). Macroscopic inactivation of Kv4.1 and Kv4.3 currents at +50 mV was described assuming the sum of two exponential terms (Fig. 11, *C* and *D*). Both fast and slow time constants were significantly reduced in the presence of elevated external K$^+$ (Kv4.1 (2 mM K$^+$): $\tau_F = 34 \pm 6$ ms, $\tau_S = 227 \pm 16$ ms, $n = 4$; Kv4.1 (98 mM K$^+$): $\tau_F = 22 \pm 2$ ms, $\tau_S = 92 \pm 7$ ms, $n = 5$; Kv4.3 (2 mM K$^+$): $\tau_F = 34 \pm 1$ ms, $\tau_S = 124 \pm 2$ ms, $n = 4$; Kv4.3 (98 mM K$^+$): $\tau_F = 29 \pm 1$ ms, $\tau_S = 105 \pm 1$ ms, $n = 4$; all differences were significant at $p < 0.05$. Also, mainly the amplitude of the fast component of Kv4.1 inactivation appeared to increase in the presence of elevated external K$^+$ (Fig. 11 *E*; $p < 0.04$). Overall, the results from all mammalian Kv4 channels are inconsistent with a C-type inactivation mechanism where the underlying conformational
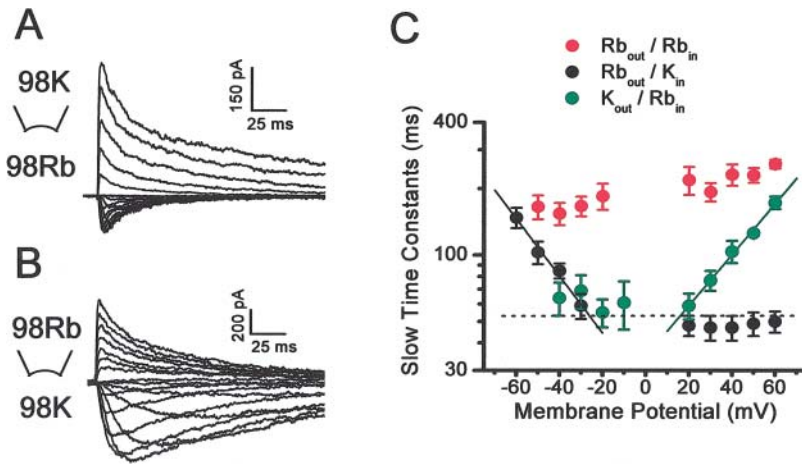
FIGURE 8 Voltage-dependence of the inactivation time constants of Rb^+ currents under bi-ionic conditions. (*A*) and (*B*) Kv4.1 currents evoked as described in Fig. 6 legend under the bi-ionic conditions indicated in the corresponding panels. Note that the currents mediated by Rb^+ exhibit slower inactivation. (*C*) Voltage-dependence of the slow time constants of inactivation. Symbols are color coded to represent three ionic conditions: red, Rb_{out}/Rb_{in}; black, Rb_{out}/K_{in}; and blue, K_{out}/Rb_{in}. Note the marked voltage-dependence that is only apparent under bi-ionic conditions. Solid lines across the symbols are the best-fit exponentials that describe the voltage-dependence of the time constants (Materials and Methods). The derived apparent charges (*q*) were 0.73 and 0.66 from the inward and outward currents mediated by Rb^+, respectively. The dashed line is the K_{out}/K_{in} average of the slow time constants measured across the indicated voltage range as demonstrated in Fig. 7.

change (responsible for increasing the relative Na^+ permeability) can be prevented by K^+ occupying an external site in the selectivity filter (Yellen, 1998, 2001; Ogielska and Aldrich, 1999; Zhou et al., 2001). On the contrary, the data suggest that when K^+ is the only permeant ion, Kv4 inactivation gating is facilitated. This effect is not likely to solely result from the hyperpolarizing shift of the *Gp-V* curve observed in the presence of elevated external K^+. Relative to 2 mM external K^+ (Beck and Covarrubias, 2001), the $V_{G=50\%}$ is leftward shifted by ~40 mV in the presence of 98 mM external K^+ (Fig. 5). The time constants of Kv4.1 inactivation in the presence of normal (2 mM; Beck and Covarrubias, 2001) and elevated external K^+ (98 mM, symmetrical conditions; Fig. 7) are weakly voltage-dependent and remained distinct even at voltages that saturate the *Gp-V* curve. For instance (at +90 mV), the τ_F values were 16 ± 2 ms (2 mM K^+; $n = 10$) and 9 ± 2 (98 mM K^+; $n = 3$); and τ_S values were 100 ± 12 ms (2 mM K^+; $n = 10$) and 63 ± 9 ms (98 mM K^+, $n = 3$).

DISCUSSION

A-type Kv4 channels are highly homologous (65–75% identity), share the putative structural elements that mediate inactivation (Jerng and Covarrubias, 1997; Jerng et al., 1999; Bähring et al., 2001), and are similarly modulated by auxiliary subunits that remodel inactivation gating (Beck et al., 2002; Holmqvist et al., 2002). Thus, it is likely that they undergo inactivation by the same mechanisms. These mechanisms appear, however, distinct from classical N-type and C-type inactivation mechanisms that are commonly observed in other Kv channels (Bähring et al., 2001; Beck and Covarrubias, 2001; Beck et al., 2002). This study has investigated the relationship between ion permeation and gating of Kv4 channels to probe their mechanisms of inactivation. The main results showed that: *1*) Rb^+ slows channel closing and, consequently, stabilizes the open state and indirectly slows inactivation from a preopen closed state;

2) Rb^+ exerts these effects only when it acts as the current carrying ion; *3*) Kv4 channels do not seem to change their ionic selectivity when they undergo inactivation; and *4*) elevated external K^+ facilitated inactivation in a manner that cannot be solely explained by a hyperpolarizing shift in voltage-dependent activation.
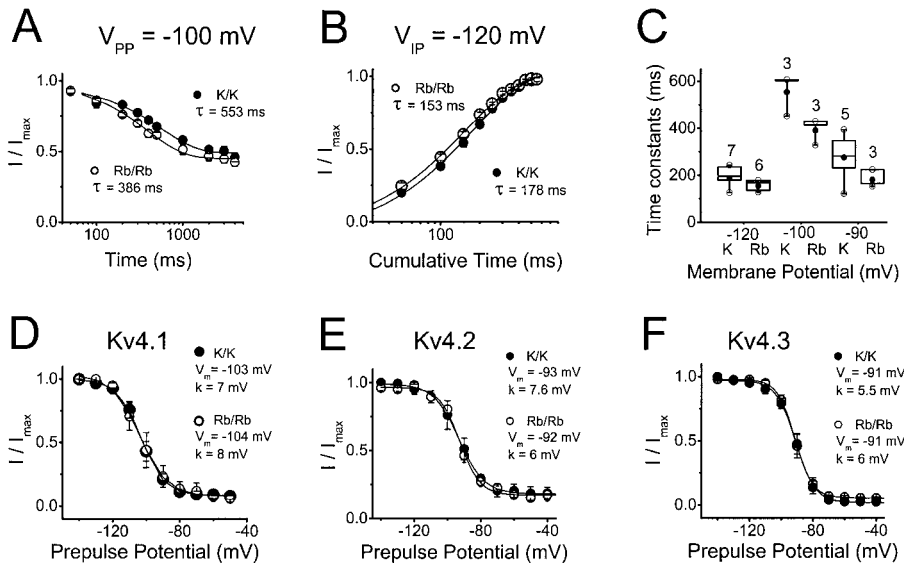
Closed-state inactivation as a preferential pathway of Kv4 inactivation

Earlier work has suggested that Kv4 channels must close before undergoing final inactivation (Jerng et al., 1999, Bähring et al., 2001; Beck and Covarrubias, 2001; Beck et al., 2002). Those results demonstrated a parallel relationship between changes in the observed rates of channel closing and inactivation. The following scheme explains how this relationship might work.

Scheme 1 represents the main gating transitions near the open state at membrane potentials that may cause maximal activation. Here, channels can inactivate from a preopen closed state and from the open state because the opening equilibrium is not strongly forward-biased. Both pathways of inactivation are voltage-independent, and the opening equilibrium is assumed to be weakly voltage-dependent ($<1\ e_0$). The opening equilibrium can affect the observed rate of inactivation in two possible ways. If $O \leftrightarrow I_O$ is the main pathway of inactivation and the $C \leftrightarrow O$ equilibrium is rapid, the time constant of inactivation can be approximated by the following equation:
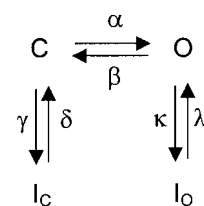
SCHEME 1

FIGURE 9 Inactivation properties of Kv4 currents mediated by K$^+$ or Rb$^+$ at hyperpolarized membrane potentials (closed-state inactivation). (A) The development of Kv4.1 inactivation at -100 mV (the midpoint of prepulse inactivation; see below) in symmetrical K$^+$ (solid symbols) or Rb$^+$ (open symbols). Peak currents evoked by step depolarizations to $+50$ mV were measured after a -100 mV prepulse of variable duration. The normalized current (I/I_{max}) is plotted against the prepulse duration. Lines represent the best-fit exponential function with the time constants indicated in the graph. (B) Recovery from inactivation of Kv4.1 channels at -120 mV in symmetrical K$^+$ (solid symbols) or Rb$^+$ (open symbols). From a two-pulse protocol, the normalized current (I/I_{max}) is plotted against the interpulse interval at -120 mV. Lines represent the best-fit exponential function with the time constants indicated in the graph. (C) Box plots (Materials and Methods) of the time constants derived from the experiments in (A) and (B). The figure above each box is the number of experiments.

At each membrane potential, the differences between the time constants in the presence of symmetrical K$^+$ or Rb$^+$ were not statistically significant ($p > 0.05$). (D–F) Voltage dependence of prepulse inactivation. Kv4.1 curves were obtained from the same patches examined in (A–C). All currents were recorded in symmetrical K$^+$ (solid symbols), or Rb$^+$ (open symbols). The voltage protocol was as described for A except that the prepulse duration was constant (10 s) and the prepulse voltage was varied (plots' ordinate). The line represents the best-fit first-order Boltzmann function with the parameters indicated in the graph. Symbols are the means from three to seven experiments.

$$\tau_{INAC} \approx \frac{1}{P_o \kappa + \lambda}, \qquad (1)$$

where P_o is the equilibrium open probability ($\alpha(\alpha + \beta)^{-1}$). If β decreases, P_o increases and, consequently, τ_{INAC} decreases (faster inactivation). Conversely, if $C \leftrightarrow I_C$ is the main pathway of inactivation and the $C \leftrightarrow O$ and $O \leftrightarrow I_O$ equilibriums are rapid, the time constant of inactivation can be approximated by the following equation:

$$\tau_{INAC} \approx \frac{1}{P_c \gamma + \delta}, \qquad (2)$$

where P_c is the equilibrium probability of being closed ($1 - P_o$). If β decreases, P_c decreases and, consequently, τ_{INAC} increases (slower inactivation). This relationship is supported by our earlier studies (Jerng et al., 1999; Beck and Covarrubias, 2001; Beck et al., 2002), which ruled unlikely open-state inactivation as the preferential pathway of inactivation in Kv4 channels.

Parallel influence of Rb$^+$ permeation on deactivation and inactivation gating

Scheme 1 predicts that any manipulations that affect the closing rate β must have a parallel effect on the development of inactivation. Independently of mutagenesis, Rb$^+$ is an ideal tool to test this hypothesis because many studies have shown that by virtue of its longer residency time in the pore of K$^+$ channels, it can stabilize the open state by hindering channel closing (e.g., Eisenman et al., 1986; Swenson and Armstrong, 1981; Demo and Yellen, 1992; Zagotta et al.,

1994). In agreement with those studies, when Rb$^+$ mediated the currents, Kv4 channels exhibited slower and weakly voltage-dependent deactivation (Figs. 1–2) and a prolonged open time (Fig. 3). Deactivation was, however, nonexponential in the presence of K$^+$ or Rb$^+$ (Fig. 2). The two observed time constants of deactivation may arise from the presence of at least two open states that were observed in single-channel records at $+60$ mV (Fig. 3). However, a nonexponential deactivation could also involve closed and/or inactivated states that the channel visits as it closes and deactivates. An interesting possibility is that the slow time constant of deactivation might in part reflect inactivation. In that case, as the channels close upon repolarization they may continue to inactivate from a closed state. Using a double pulse protocol to test the available current as the channels deactivate at -120 mV, the data clearly showed that Kv4.1 channels undergo limited time-dependent inactivation from which they subsequently recover (40% inactivation before recovery becomes apparent; data not shown). This inactivation process was also slowed and had a smaller magnitude when Rb$^+$ mediated the tail current. These observations demonstrate a pathway of inactivation that is coupled to channel closing ($O \rightarrow C \rightarrow I$). Thus, when Rb$^+$ slowed channel closing the observed rate of inactivation is slowed too and the amplitude ratio (A_F/A_S) of the biexponential function that describes the tail current decreases as the slow component becomes more prominent.

Although the main amplitude of the unitary Rb$^+$ currents was reduced (Table 2) as a consequence of a tighter interaction of Rb$^+$ in the selectivity filter (Eisenman et al., 1986; Morais-Cabral et al., 2001), the peak Rb$^+$ currents were significantly larger than the corresponding K$^+$ currents
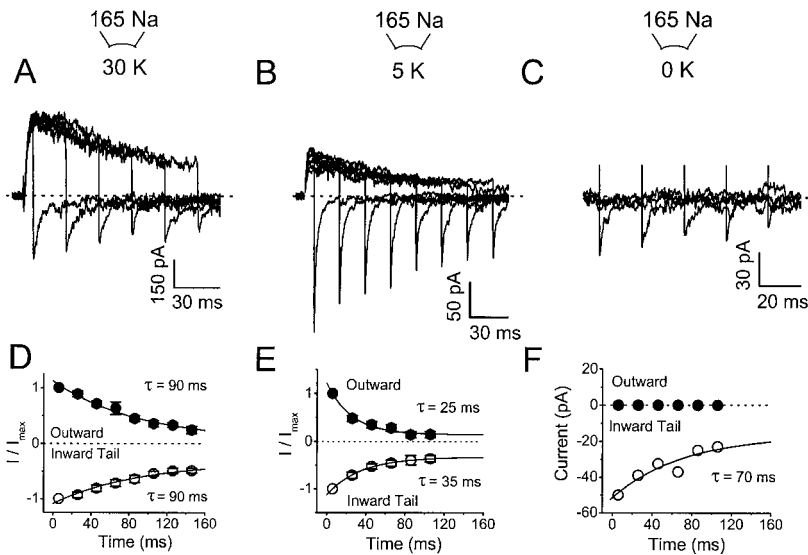
FIGURE 10 The relative Na^+ permeability of Kv4.1 channels is not altered during the development of inactivation. (*A*–*C*) Outward (K^+) and inward (Na^+) currents evoked by a step depolarization to +50 mV followed by hyperpolarizing step to −140 mV, from a holding potential of −100 mV. The duration of the depolarizing pulse is increased in 20-ms increments. The intracellular solutions (Materials and Methods) contained 30 mM KCl (*A*), 5 mM (*B*), and 0 KCl (*C*) (no added KCl). (*D*)–(*F*) Normalized outward (at the end of the depolarizing pulse) and inward tail currents (peaks) are plotted against the duration of the depolarizing pulse. Lines represent the best-fit exponential functions with the time constants indicated in the graphs. The symbols are mean values of six to seven experiments (except *F*, which is the result of a representative experiment; see text).

(Fig. 4). Rb^+ also induced a modest hyperpolarizing shift of the normalized peak *G-V* relation (Fig. 5 *C*). However, such a shift is not sufficient to explain the enhanced currents at voltages where the peak *G-V* curves tend to plateau. A plausible explanation needs to take into account the low maximum open probability of Kv4 channels (as a result of a weakly forward-biased or backward-biased opening step; $\alpha \leq \beta$ in Scheme 1). Earlier studies have supported this hypothesis (Jerng et al., 1999; Bähring et al., 2001; Beck and Covarrubias, 2001; Beck et al., 2002). Rb^+ might affect weakly voltage-dependent and voltage-independent steps that directly influence the stability of the open state. Thus, Rb^+ may increase the maximum open probability by slowing the closing rate. Interestingly, the increase of the peak Kv4.1 current by Rb^+ was larger than that of Kv4.2 and Kv4.3; but the Kv1.3 peak current was, by contrast, reduced (despite slower closing of the Kv1.3 Rb^+ current; data not shown). In combination with a reduced unitary Rb^+ current, whether the peak Rb^+ current is increased or decreased when the closing rate is decreased depends on the relationship between the opening and closing rates. If $\alpha \leq \beta$ (backward-biased or not strongly forward-biased), reducing β can have a significant impact on the maximum open probability. Thus, because this relationship might differ quantitatively among Kv4 channels, the degree by which Rb^+ enhances the currents differs. Conversely, if $\alpha \gg \beta$ (strongly forward-biased), reducing β might have little impact on the open probability. Therefore, the macroscopic current amplitude is more likely to be mainly determined by the unitary current amplitude. The latter might apply to Kv1.3 and other *Shaker* K^+ channels, which exhibit a strongly forward-biased opening equilibrium (Zagotta et al., 1994; Schoppa and Sigworth, 1998; Ledwell and Aldrich, 1999).

It could be argued that Rb^+ also stabilizes the open state by directly slowing inactivation from the open state. However, our earlier studies have suggested a limited role of open-state inactivation in Kv4 channels (Jerng and Covarrubias, 1997; Jerng et al., 1999; Bähring et al., 2001; Beck and Covarrubias, 2001; Beck et al., 2002). Other experiments reported here ruled unlikely a simple "foot-in-the-door" mechanism (Yeh and Armstrong, 1978; Swenson and Armstrong, 1981; Lopez-Barneo et al., 1993) to explain the main effects of Rb^+ on Kv4 inactivation as the result of a direct interaction. First, elevated external K^+ facilitates inactivation gating (Fig. 11) independently of a hyperpolarizing shift. Second, Rb^+ does not significantly affect closed-state inactivation (Fig. 9). By contrast, in *Shaker* K^+ channels, elevated external K^+ appears to slow both open-state and closed-state inactivation and thereby enhances the peak currents (Pardo et al., 1992; Lopez-Barneo et al., 1993).

Thus, having established the viability of the Rb^+ paradigm in Kv4 channels, the main drive of this study was to investigate the presence of preferential inactivation from the preopen closed state by testing whether Rb^+ might similarly influence deactivation and inactivation in all Kv4 channels. Importantly, inactivation appeared slower only when Rb^+ mediates the current (Figs. 6–8), and the slow time constant of inactivation of the Rb^+ currents exhibited novel voltage-dependence (Figs. 7 and 8). Under the bi-ionic conditions of these experiments, this voltage-dependence clearly shows how membrane polarization influences inactivation gating through its effect on ion permeation. Channel closing is slowed as Rb^+ predominantly occupies the multi-ion pore and, consequently, slows inactivation from the preopen closed state (both in the inward and outward directions; Fig. 8). Interestingly, the fast time constant of inactivation is also slowed to some extent (Fig. 7). However, if $\gamma \geq \kappa$ in Scheme 1, the observed two time constants of inactivation cannot be distinctly associated with specific equilibriums (i.e., open state versus closed state inactivation). Kinetic modeling has suggested that γ and κ are probably similar for Kv4 channels in inside-out patches (Beck and Covarrubias,
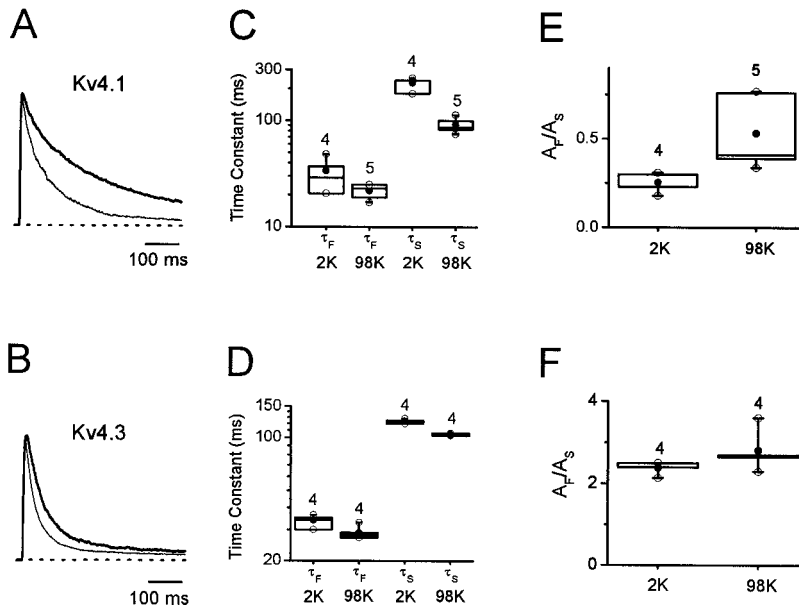
FIGURE 11 The effect of elevated external K$^+$ on inactivation of Kv4 channels. Outward Kv4.1 (*A*) and Kv4.3 (*B*) currents evoked by a step depolarization from −100 to +50 mV in the presence of normal external K$^+$ (2 mM; *thick line*) or elevated external K$^+$ (98 mM; *thin line*). All currents were recorded from cell-attached *Xenopus* oocyte macropatches. (*C*) and (*D*) Corresponding box plots (Materials and Methods) of the fast and slow time constants of the development of inactivation at +50 mV in normal external K$^+$ (2 mM) and elevated external K$^+$ (98 mM). (*E*) and (*F*) Corresponding amplitude ratios A_F/A_S of the biexponential fits. The number of experiments is given above the boxes.

2001). Thus, inactivation from the preopen closed state also influences the observed fast time constant of the development of inactivation. This effect discouraged a mechanistic interpretation of the amplitude ratio A_F/A_S derived from the biexponential fits of macroscopic inactivation (Fig. 7). Additionally, a more quantitative analysis of this ratio was hampered by its significant variability (Fig. 7, *D–F*). Overall, the qualitatively similar effects of Rb$^+$ on all Kv4 channels support the idea of common mechanisms of inactivation in these channels. By maintaining a low open probability and inactivating from the preopen closed state, Kv4 channels act as moderators that fine-tune excitability without exerting a terminal effect on the neuronal and cardiac action potentials or neuronal subthreshold depolarizations. It is also significant that preopen closed-state inactivation is the preferential pathway of inactivation, and recovery from inactivation does not involve channel reopening. These features allow electrically silent and rapid repriming of the Kv4 current.

Can a structural change at an external site in the selectivity filter explain Kv4 inactivation?

An important hallmark of C-type inactivation in Kv channels is an apparent pore constriction at the outer mouth of the selectivity filter, also referred to as the P-type component of C-type inactivation (reviewed by Yellen, 1998; 2001). In agreement with this idea, when certain Kv channels undergo C-type inactivation they become relatively more permeable to Na$^+$ (Starkus et al., 1997, 2000; Kiss et al., 1999). If the external pore diameter is reduced during C-type inactivation, the relative Na$^+$ permeability might increase because K$^+$ ions are too large to fit in the pore and Na$^+$ ions may now experience a better low-energy fit (Doyle et al., 1998). This

scenario, however, does not seem to take place in Kv4 channels. In the absence of inactivation, Kv4.1 channels are permeable to Na$^+$ (when external Na$^+$ is the only permeant ion), but the peak tail Na$^+$ currents just mirror the development of inactivation (with no added internal K$^+$ or in the presence of low internal K$^+$; Fig. 10). This observation implies that an external site in the selectivity filter does not undergo a significant structural change that could improve the channel's relative Na$^+$ permeability during inactivation. Frazier et al., (2000) demonstrated that the whole-cell results from Kiss et al., (1999) could be influenced by a current-dependent depletion of internal K$^+$. In our experiments with inside-out patches the presence of a similar complication is unlikely because the currents studied in Fig. 10 were relatively small and the reversal potentials were not affected by inactivation. The presence of residual tail Na$^+$ currents that followed prolonged depolarizations (Fig. 10, *A* and *B*) is most likely the result of incomplete inactivation. Reopening during recovery from open-state inactivation might also contribute to these currents (Ruppersberg et al., 1991; Demo and Yellen, 1991), but other studies have failed to demonstrate the presence of such a reopening in Kv4 channels (Jerng and Covarrubias, 1997; Bähring et al., 2001). More experiments are necessary to gain further insights into the nature of the persistent Na$^+$ tail current.

The distinct effect of elevated K$^+$ on the development of Kv4 inactivation also rendered C-type inactivation in Kv4 channels unlikely (Fig. 11). In *Shaker* K$^+$ channels, elevated external K$^+$ prevents C-type inactivation (i.e., a pore constriction) by a "foot-in-the-door" mechanism at an external site (Lopez-Barneo et al., 1993; Yellen, 1998; Ogielska and Aldrich, 1999). By contrast, how can elevated external K$^+$ favor inactivation in Kv4 channels? External Na$^+$ does not cause slower inactivation under normal ionic

conditions (2 mM K^+). When Na^+ was fully replaced with nonpermeant $NMDG^+$ (with 2 mM K^+) the development of inactivation remained unaffected (data not shown). We hypothesize that stabilization of the selectivity filter by elevated external K^+ may facilitate a conformational change that mediates inactivation at an internal site (even when the channel is closed). This modulation implies a more direct effect of K^+ on inactivation from the preopen closed state, which is distinct from the indirect modulation that depends on the slowing of channel closing by Rb^+, as explained above.

The apparent absence of C-type inactivation in all Kv4 channels might be explained by their specific pore structure. In all known *Shal* channels, valine occupies the site that corresponds to threonine 449 in *Shaker* K^+ channels. Mutation of this residue to valine in *Shaker* K^+ channels virtually eliminates C-type inactivation (Lopez-Barneo et al., 1993). Also, serine (polar) occupies another critical S6 position, which corresponds to alanine or valine (nonpolar) in *Shaker* B and Kv1 channels (alanine 463 in *Shaker* B; Hoshi et al., 1991). This site appears to control the K^+ affinity at an internal pore site (Ogielska and Aldrich, 1998; 1999). Especially important might be the presence of tyrosine at the position corresponding to tryptophan 435 in *Shaker* B. This tryptophan is highly conserved in Kv channels and KcsA bacterial channels (Doyle et al., 1998), and the W434F mutation at the neighboring highly conserved tryptophan introduces steady-state C-type inactivation in *Shaker* K^+ channels (Perozo et al., 1993; Yang et al., 1997; Starkus et al., 1998; but see Olcese et al., 1997). Thus, a distinct pore structure hindering C-type inactivation in Kv4 channels might have allowed other mechanisms of inactivation to evolve.

REFERENCES

Baukrowitz, T., and G. Yellen. 1995. Modulation of K^+ current by frequency and external $[K^+]$: a tale of two inactivation mechanisms. *Neuron*. 15:951–960.

Bähring, R., J. Dannenberg, H. C. Peters, T. Leicher, O. Pongs, and D. Isbrandt. 2001. Kinetic analysis of open- and closed-state inactivation transitions in human Kv4.2 A-type potassium channels. *J. Physiol. (Lond.)*. 535:65–81.

Beck, E. J., and M. Covarrubias. 2001. Kv4 channels exhibit modulation of closed-state inactivation in inside-out patches. *Biophys. J.* 81:867–883.

Beck, E. J., M. Bowlby, W. F. An, K. Rhodes, and M. Covarrubias. 2002. Remodeling inactivation gating of Kv4 channels by KChIP1, a small-molecular-weight calcium binding protein. *J. Physiol. (Lond.)*. 538:691–706.

Chen, P. S. F., D. Steele, and D. Fedida. 1997. Allosteric effects of permeant cations on gating currents during K^+ channel deactivation. *J. Gen. Physiol.* 110:87–100.

Covarrubias, M., M. Shahidullah, E. J. Beck, and H. H. Jerng. 2000. Biophysical and molecular evidence of novel mechanisms of inactivation gating in Kv4 channels. *Biophys. J.* 78:213A.

Demo, S. D., and G. Yellen. 1991. The inactivation gate of the *Shaker* K^+ channel behaves like an open-channel blocker. *Neuron*. 7:743–753.

Demo, S. D., and G. Yellen. 1992. Ion effects on gating of the Ca^{2+}-activated K^+ channel correlate with occupancy of the pore. *Biophys. J.* 61:639–648.

Ding, S., and R. Horn. 2002. Tail end of the S6 segment: role in permeation in *Shaker* potassium channels. *J. Gen. Physiol.* 120:87–97.

Doyle, D. A., C. J. Morais, R. A. Pfuetzner, A. Kuo, J. M. Gulbis, S. L. Cohen, B. T. Chait, and R. MacKinnon. 1998. The structure of the potassium channel: molecular basis of K^+ conduction and selectivity. *Science*. 280:69–77.

Eghbali, M., R. Olcese, M. Zarei, L. Toro, and E. Stefani. 2001. External K^+ ion increases the rate of inactivation of Kv4.3 K^+ channels. *Biophys. J.* 80:444A.

Frazier, C. J., E. G. George, and S. W. Jones. 2000. Apparent change in ion selectivity caused by changes in intracellular K^+ during whole-cell recording. *Biophys. J.* 78:1872–1880.

Eisenman, G., R. Latorre, and C. Miller. 1986. Multi-ion conduction and selectivity in the high-conductance Ca^{++}- activated K^+ channel from skeletal muscle. *Biophys. J.* 50:1025–1034.

Gomez-Lagunas, F., and C. M. Armstrong. 1994. The relation between ion permeation and recovery from inactivation of *Shaker* B K^+ channels. *Biophys. J.* 67:1806–1815.

Holmqvist, M. H., J. Cao, R. Hernandez-Pineda, M. D. Jacobson, K. I. Carroll, M. A. Sung, M. Betty, P. Ge, K. J. Gilbride, M. E. Brown, M. E. Jurman, D. Lawson, I. Silos-Santiago, Y. Xie, M. Covarrubias, K. J. Rhodes, P. S. Distefano, and W. F. An. 2002. Elimination of fast inactivation in Kv4 A-type potassium channels by an auxiliary subunit domain. *Proc. Natl. Acad. Sci. USA*. 99:1035–1040.

Hoshi, T., W. N. Zagotta, and R. W. Aldrich. 1991. Two types of inactivation in *Shaker* K^+ channels: effects of alterations in the carboxy-terminal region. *Neuron*. 7:547–556.

Jerng, H. H., and M. Covarrubias. 1997. K^+ channel inactivation mediated by the concerted action of the cytoplasmic N- and C-terminal domains. *Biophys. J.* 72:163–174.

Jerng, H. H., M. Shahidullah, and M. Covarrubias. 1999. Inactivation gating of Kv4 potassium channels: molecular interactions involving the inner vestibule of the pore. *J. Gen. Physiol.* 113:641–660.

Kirichok, Y. V., A. V. Nikolaev, and O. A. Krishtal. 1998. $[K^+]$ out accelerates inactivation of Shal-channels responsible for A-current in rat CA1 neurons. *Neuroreport*. 9:625–629.

Kiss, L., J. LoTurco, and S. J. Korn. 1999. Contribution of the selectivity filter to inactivation in potassium channels. *Biophys. J.* 76:253–263.

Ledwell, J. L., and R. W. Aldrich. 1999. Mutations in the S4 region isolate the final voltage-dependent cooperative step in potassium channel activation. *J. Gen. Physiol.* 113:389–414.

Levy, D. I., and C. Deutsch. 1996a. Recovery from C-type inactivation is modulated by extracellular potassium. *Biophys. J.* 70:798–805.

Levy, D. I., and C. Deutsch. 1996b. A voltage-dependent role for K^+ in recovery from C-type inactivation. *Biophys. J.* 71:3157–3166.

Liu, Y., M. E. Jurman, and G. Yellen. 1996. Dynamic rearrangement of the outer mouth of a K^+ channel during gating. *Neuron*. 16:859–867.

Loots, E., and E. Y. Isacoff. 1998. Protein rearrangements underlying slow inactivation of the *Shaker* K^+ channel. *J. Gen. Physiol.* 112:377–389.

Lopez-Barneo, J., T. Hoshi, S. H. Heinemann, and R. W. Aldrich. 1993. Effects of external cations and mutations in the pore region on C-type inactivation of *Shaker* potassium channels. *Receptors Channels*. 1:61–71.

Matteson, D. R., and R. P. J. Swenson. 1986. External monovalent cations that impede the closing of K^+ channels. *J. Gen. Physiol.* 87:795–816.

Morais-Cabral, J. H., Y. Zhou, and R. Mackinnon. 2001. Energetic optimization of ion conduction rate by the K$^+$ selectivity filter. *Nature.* 414:37–42.

Ogielska, E. M., W. N. Zagotta, T. Hoshi, S. H. Heinemann, J. Haab, and R. W. Aldrich. 1995. Cooperative subunit interactions in C-type inactivation of K channels. *Biophys. J.* 69:2449–2457.

Ogielska, E. M., and R. W. Aldrich. 1998. A mutation in S6 of *Shaker* potassium channels decreases the K$^+$ affinity of an ion binding site revealing ion-ion interactions in the pore. *J. Gen. Physiol.* 112: 243–257.

Ogielska, E. M., and R. W. Aldrich. 1999. Functional consequences of a decreased potassium affinity in a potassium channel pore. Ion interactions and C-type inactivation. *J. Gen. Physiol.* 113:347–358.

Olcese, R., R. Latorre, L. Toro, F. Bezanilla, and E. Stefani. 1997. Correlation between charge movement and ionic current during slow inactivation in *Shaker* K$^+$ channels. *J. Gen. Physiol.* 110:579–589.

Panyi, G., Z. Sheng, and C. Deutsch. 1995. C-type inactivation of a voltage-gated K$^+$ channel occurs by a cooperative mechanism. *Biophys. J.* 69:896–903.

Pardo, L. A., S. H. Heinemann, H. Terlau, U. Ludewig, C. Lorra, O. Pongs, and W. Stuhmer. 1992. Extracellular K$^+$ specifically modulates a rat brain K$^+$ channel. *Proc. Natl. Acad. Sci. USA.* 89:2466–2470.

Perozo, E., R. MacKinnon, F. Bezanilla, and E. Stefani. 1993. Gating currents from a nonconducting mutant reveal open-closed conformations in *Shaker* K$^+$ channels. *Neuron.* 11:353–358.

Ruppersberg, J. P., R. Frank, O. Pongs, and M. Stocker. 1991. Cloned neuronal IK(A) channels reopen during recovery from inactivation. *Nature.* 353:657–660.

Sala, S., and D. R. Matteson. 1991. Voltage-dependent slowing of K$^+$ channel closing kinetics by Rb$^+$. *J. Gen. Physiol.* 98:535–554.

Schoppa, N. E., and F. J. Sigworth. 1998. Activation of *Shaker* potassium channels. I. Characterization of voltage-dependent transitions. *J. Gen. Physiol.* 111:271–294.

Shahidullah, M., and M. Covarrubias. 2001. The ionic and kinetic basis of slow inactivation in neuronal and cardiac Kv4 channels: the "occupancy hypothesis" revisited. *Biophys. J.* 80:438A.

Starkus, J. G., L. Kuschel, M. D. Rayner, and H. S. Heinemann. 1998. Macroscopic Na$^+$ currents in the "nonconducting" *Shaker* potassium channel mutant W434F. *J. Gen. Physiol.* 112:85–93.

Starkus, J. G., L. Kuschel, M. D. Rayner, and S. H. Heinemann. 1997. Ion conduction through C-type inactivated *Shaker* channels. *J. Gen. Physiol.* 110:539–550.

Starkus, J. G., S. H. Heinemann, and M. D. Rayner. 2000. Voltage dependence of slow inactivation in *Shaker* potassium channels results from changes in relative K$^+$ and Na$^+$ permeabilities. *J. Gen. Physiol.* 115:107–122.

Swenson, R. P. J., and C. M. Armstrong. 1981. K$^+$ channels close more slowly in the presence of external K$^+$ and Rb$^+$. *Nature.* 291:427–429.

Townsend, C., A. H. Hartmann, and R. Horn. 1997. Anomalous effect of permeant ion concentration on peak open probability of cardiac Na$^+$ channels. *J. Gen. Physiol.* 110:11–21.

Yeh, J. Z., and C. M. Armstrong. 1978. Immobilisation of gating charge by a substance that simulates inactivation. *Nature.* 273:387–389.

Yellen, G. 1998. The moving parts of voltage-gated ion channels. *Q. Rev. Biophys.* 31:239–295.

Yellen, G. 2001. Keeping K$^+$ completely comfortable. *Nat. Struct. Biol.* 8:1011–1013.

Yang, Y., Y. Yan, and F. J. Sigworth. 1997. How does the W434F mutation block current in *Shaker* potassium channels? *J. Gen. Physiol.* 109:779–789.

Zagotta, W. N., T. Hoshi, J. Dittman, and R. W. Aldrich. 1994. *Shaker* potassium channel gating. II. Transitions in the activation pathway. *J. Gen. Physiol.* 103:279–319.

Zheng, J., and F. J. Sigworth. 1997. Selectivity changes during activation of mutant *Shaker* potassium channels. *J. Gen. Physiol.* 110:101–117.

Zheng, J., L. Vankataramanan, and F. J. Sigworth. 2001. Hidden Markov model analysis of intermediate gating steps associated with the pore gate of *Shaker* potassium channels. *J. Gen. Physiol.* 118:547–564.

Zhou, Y., J. H. Morais-Cabral, A. Kaufman, and R. Mackinnon. 2001. Chemistry of ion coordination and hydration revealed by a K$^+$ channel-Fab complex at 2.0 Å resolution. *Nature.* 414:43–48.